

Tactile Rendering Using Three Basic Stimulus Components in Ultrasound Midair Haptics

Tao Morisaki, Atsushi Matsubayashi, Yasutoshi Makino, and Hiroyuki Shinoda, *Member, IEEE*

Abstract—Ultrasound midair haptics (UMH) can present non-contact tactile stimuli using focused ultrasound without restricting the user’s movement. Recently, UMH has been shown to present not only conventional vibrotactile sensations but also static pressure sensations by locally rotating an ultrasound focus at several hertz. With these pressure and vibration sensations, UMH covers three mechanoreceptors on which tactile perception relies: SA-I, FA-I, and FA-II. This study proposes a texture rendering method in UMH based on these receptor characteristics. Three basic ultrasonic stimuli corresponding to each mechanoreceptor are designed, and tactile textures are rendered through their combinations. For SA-I, a pressure stimuli were employed. For FA-I and FA-II, vibration stimuli at 30 Hz and 150 Hz, respectively, are employed. Experimental results demonstrate that the proposed method can render at least six discriminable textures with different roughness and friction sensations. Notably, through comparisons with real physical objects, we found that the pressure-only stimulus was perceived as slippery and smooth. Its smoothness was similar to a glass-marble. When vibration stimuli were synthesized, the perceived roughness and friction increased significantly. The roughness level reached that of a 100-grit sandpaper.

Index Terms—Midair haptics, texture, vibration sensation, and pressure sensation.

I. INTRODUCTION

Ultrasound midair haptics, which presents a non-contact tactile stimulus without restricting the user’s body movement [1], [2], [3], is a promising haptic technology. By focusing ultrasound onto the skin, a non-contact force called acoustic radiation force is generated at the focus [4], conveying tactile sensation. Since this method does not require users to wear mechanical devices, it provides a natural and immersive tactile experience. Ultrasound midair haptics has been used for many applications [5], including midair interfaces with tactile feedback [6], [7], [8], [9], behavioral guidance [10], [11], [12], and evoking pleasant sensations [13].

The reproduction of real object texture has also been actively studied in midair haptics [14], [15], [16], [17], [18]. Sakiyama et al. measured changes in pressure distribution on the skin generated by the stroking of real objects and reproduced them using focused ultrasound [16]. Ablart et al. reported roughness sensations were evoked by rotating an

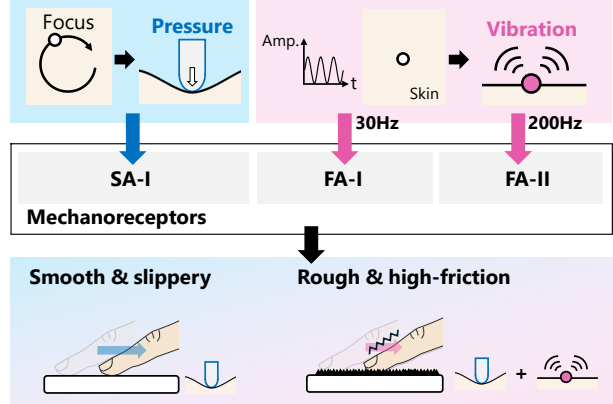


Fig. 1. Proposed tactile rendering method, synthesizing three ultrasound stimuli primarily stimulating different mechanoreceptors. For SA-I, a 5 Hz focus rotation, evoking a static pressure sensation was used. For FA-I and FA-II, vibration stimuli at 30 and 150 Hz was used, respectively. Pressure-only stimulus was perceived as slippery and smooth. When vibration sensations were synthesized, the perceived roughness and friction increased.

ultrasound focus on the palm, and the roughness sensation was varied when the focus rotation frequency was varied [15].

However, perceptual mechanisms-based tactile rendering has been challenging in ultrasound midair haptics, as a static pressure stimulus, a basic stimulus component, has been lacking. Human’s texture perception partly relies on the responses of mechanoreceptors with different frequency characteristics: SA-I, (Slowly adaptive type-I), FA-I, and FA-II (Fast adaptive type-I and II) [19]. FA-I and FA-II primarily respond to vibrations around 30 Hz and 150 Hz, respectively, while SA-I primarily responds to static pressure. Considering this mechanism, synthesizing three types of stimuli corresponding to each receptor is effective for texture reproduction, and this approach has already been adopted in other haptic displays [20], [21], [22]. In midair haptics, vibration stimuli around 30 and 150 Hz can be presented by modulating the amplitude of ultrasound. In contrast, static pressure stimulus corresponding to SA-I have not been achievable, as the radiation force of ultrasound is weak, several tens of millinewtons. Without pressure stimulus, for example, an ideal smooth and slippery texture cannot be rendered, since vibration sensation evokes roughness and friction sensations [23], [24], [25], [26].

To address this issue, Morisaki et al. recently demonstrated that moving an ultrasound focus at a few hertz evokes a static pressure sensation [27], [28], [29]. In their experiment, the focus rotated at 5 Hz along a circular trajectory with a radius of several millimeters and the perceived intensity was equivalent to approximately 0.2 N, ten times stronger than

Manuscript received xx; revised xx.

This work was supported in part by NEDO SIP 23201554-0 and JSPS KAKENHI 25K21261.

T. Morisaki is with the Communication Science Laboratories, NTT, Inc., Atsugi, Japan. E-mail: tao.morisaki@ntt.com

A. Matsubayashi, Y. Makino, and H. Shinoda are with the Graduate School of Frontier Sciences, the University of Tokyo, Kashiwa-shi, Chiba, 277-8561, Japan (E-mail: matsubayashi@hapis.k.u-tokyo.ac.jp; yasutoshi_makino@k.u-tokyo.ac.jp; hiroyuki_shinoda@k.u-tokyo.ac.jp).

the radiation force [28]. Because the response of FA-I and FA-II elicits the vibration sensation, whereas that of SA-I elicits a pressure sensation, the 5 Hz focus rotation is an effective method to primarily stimulate SA-I. The pressure stimulus enable to design of stimuli corresponding to each mechanoreceptor frequency characteristic using ultrasound.

In this study, we propose a texture rendering method, synthesizing three ultrasound stimuli stimulating different mechanoreceptors primarily, and investigate the renderable texture. For SA-I, we employed a 5 Hz focus rotation, evoking a static pressure sensation. For FA-I and FA-II, we employed vibration stimuli at 30 and 150 Hz, respectively. These vibration stimuli were synthesized to the pressure stimulus by modulating the amplitude of the focus rotating at 5 Hz.

In the experiments, we demonstrated that the proposed method can render at least six distinguishable textures with different roughness and friction sensations. The roughness and friction sensations of the ultrasound stimuli were evaluated by comparing them with real physical objects. Notably, when only the pressure stimulus was presented, the resulting sensation was perceived as highly slippery and smooth. Its smoothness level was close to that of a glass marble. When vibration sensations were synthesized, the perceived roughness and friction increased significantly. The roughness level reached that of a 100 grit sandpaper. Although previous studies have presented smooth and rough sensations using focused ultrasound, those approaches did not employ static pressure stimuli and did not conduct a comparison with real materials [15], [30]. They reported the relative roughness score (magnitude) only.

II. RELATED WORKS

A. Contact-type Haptic Display

In contact-type haptic displays, as our approach, synthesizing multiple stimuli to which different mechanoreceptor primarily respond have been proposed to render tactile textures. Konyo et al. simultaneously presented 5 Hz vibration and higher frequency vibrations using a single vibrator [20]. The 5 Hz vibration stimulus corresponds to the role of our LM stimulus. They reported that a 5 Hz vibration evoked a static pressure sensation [20]. Yem et al. simultaneously presented pressure sensation and low-frequency vibration sensation using electrical stimulation [21]. They also simultaneously presented higher-frequency vibration sensation and shear force stimulation using a DC motor. Huang et al. developed a thin haptic device with built-in soft electrodes and electromechanical actuators [22]. The electrodes presented pressure sensation and low-frequency vibration, while the actuators presented high-frequency vibration.

These studies employed contact-type haptic displays, whereas our study used non-contact ultrasound stimuli.

B. Ultrasound Midair Haptics

Our study proposes to synthesize pressure and vibration sensations in ultrasound midair haptics and evaluate its performance on tactile texture rendering. Here, we introduce previous studies on rendering haptic textures using ultrasound. Sakiyama et al. measured the spatiotemporal distribution of

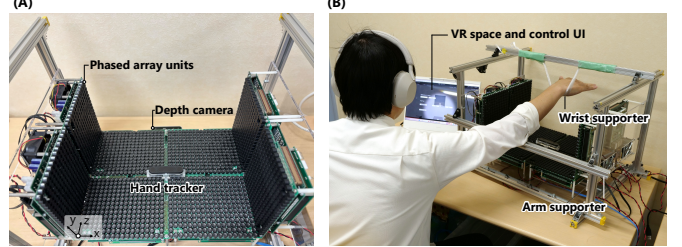


Fig. 2. Ultrasound tactile display system. This system was used in Experiment 1–4. (A) Hardware setup. (B) A photo of a participant using the system.

pressure when stroking soft real objects on a two-dimensional pressure sensor and reproduced the pressure distribution using focused ultrasound [16]. Hosoi et al. rendered voluminous fur sensation using STM stimulus [18]. They modeled the pressure pattern when stroking fur, and adjusted the movement frequency and intensity of the STM based on the model. Ablart et al. reported that in STM stimuli, in which an ultrasound focus rotates palm-sized, the roughness sensation was varied, related to the movement frequency and trajectory length [15]. Using the STM method, Beattie et al. generated ultrasound roughness stimuli from visual texture images [30]. Freeman showed that the roughness of the STM was enhanced by modulating the amplitude of the rotating focus with white noise [17]. Freeman et al. rendered macro-scale roughness textures by dynamically changing focus position [14]. With their method, a focus position was moved between a virtual surface, such as an arranged convex surface, and the user's hand. Multi-modal approach was also proposed [31], [32]. Montano et al. evaluated the effect of auditory stimulus on perception of texture rendered by ultrasound [31]. Xue et al. rendered fabric texture simultaneously use ultrasound tactile stimuli and auditory stimuli and evaluated their roughness [32]. In addition to these rendering specific haptic sensations, general stimulus design frameworks have also been proposed [33], [34], [35].

These studies did not use pressure sensation to render haptic texture. This paper is the first to synthesize pressure and vibration sensations to render textures with different roughness and friction sensations using ultrasound stimuli. As an exception, Morisaki et al. proposed a concept of synthesizing pressure and vibration sensations [36]; however, they did not evaluate its performance.

III. EXPERIMENTAL SETUP

A. Overview

This ultrasound tactile display system, shown in Fig. 2, was used in all experiments conducted in this study. Fig. 3 shows an overview of the provided tactile experience. The user's 3D hand model and a spherical virtual object were presented on a PC display. Users can control the hand model by moving their real hand. When the hand model touched the virtual object, a tactile stimulus was presented to the user's real hand.

The tactile display system consists of eight ultrasound phased array units [37], a hand tracker (Leap Motion 2, Ultraleap, Ltd.), a depth camera (RealSense D415, Intel), and a

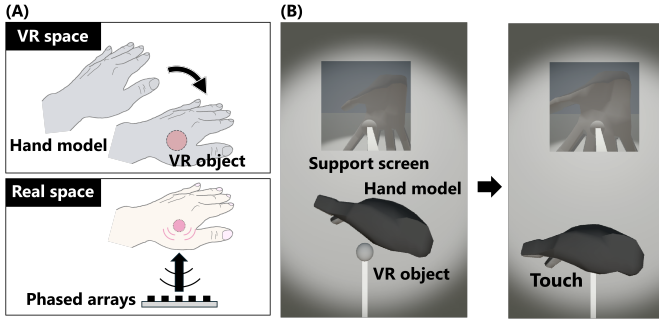


Fig. 3. Tactile experience provided by our tactile display system. (A) Schematic illustration. When touching a spherical VR object with a hand model, a tactile stimulus was presented to the contact position at the real hand. (B) Screenshot of the VR object and hand model. The support screen displayed images from beneath the hand, helping participants touch VR objects.

control PC. The coordinate system of the tactile display system is shown in Fig. 2.

An ultrasound phased array, an array of individually controllable ultrasound transducers, was used to present tactile stimuli. A phased array can generate an ultrasound focus at arbitrary three-dimensional positions by controlling the phase of each transducer [2], [3]. A total of 1,992 transducers were used, with an emitted ultrasound frequency of 40 kHz [37].

The hand tracker and the depth camera were used to determine the timing and position for presenting ultrasound stimuli. The depth camera was used to present the ultrasound focus accurately on the surface of the hand using the obtained depth data. First, the hand tracker detected the participant's hand and generated a hand model. When the hand model touched a spherical VR object, the y-position of the real hand y^{hand} at the contact position was measured with the depth camera. Based on the detected y-position, the center position of the ultrasound stimulus p^c was determined as follows:

$$p^c = (x^c, y^{hand}, z^c), \quad (1)$$

where x^c and z^c are the x and z positions of the spherical VR objects' center. This measurement process ran at 90 Hz.

B. Stimulus Design

This section describes the stimulus design to synthesize pressure and vibration sensations. A schematic of the stimulus design is shown in Fig. 4A and B. First, to present a pressure sensation, we used an LM stimulus [27]. In the LM, five ultrasound foci were simultaneously presented and rotated since such multiple foci rotation is more suitable for producing static pressure sensation [28]. The previous study reported that a non-static sensation, such as a perception of focused movement, was suppressed using a multi-foci condition compared with a single focus rotation condition [28]. The multiple foci rotation has also been used in STM, but these studies did not aim to present static pressure sensations [38], [39]. To synthesize vibration sensation with the pressure sensation, the amplitude of these five foci was modulated with sinusoidal waves of 30 and 150 Hz. We also used a composite wave of 30 and 150 Hz waves as a modulation waveform. Hajas et al. have used a similar method, amplitude-modulated STM stimulus;

however, they aimed to render 2D tactile shapes and not to simultaneously present pressure and vibration sensations [40].

1) *Formulation*: We first formulate the five foci trajectory of LM p_i^{LM} . The $i \in \{1, \dots, 5\}$ is the focus number simultaneously presented in the LM. The $p_i^{LM}(t) = (x_i^{LM}, y_i^{LM}, z_i^{LM})$ is as follows:

$$x_i^{LM} = x^c + r \cos(2\pi f^{LM} t + \phi^{LM}), \quad (2)$$

$$y_i^{LM} = y^{hand}, \quad (3)$$

$$z_i^{LM} = z^c + r \sin(2\pi f^{LM} t + \phi^{LM}), \quad (4)$$

$$\phi^{LM} = \frac{d}{2r} \quad (5)$$

where f^{LM} [Hz] is the focus rotation frequency, r [mm] is the radius of the focus trajectory, and d [mm] is the space of simultaneously presented multiple foci. The foci positions were updated at 1000 Hz.

The driving signal of each transducer was calculated using a linear synthesis scheme as in the previous study [28]. The driving signal s for a single transducer is as follows:

$$s = Ae^{(2\pi ft - \sum_i^N \phi_i)}, \quad (6)$$

where t is the elapsed time, j is the imaginary unit, $f = 40$ kHz is the frequency of ultrasound, and A is the driving amplitude of the transducer. ϕ_i is the phase for creating i -th focus in LM and $N = 5$ is the foci number.

Second, we formulate the modulation of transducer amplitude for presenting vibration sensation. All transducers were driven with the same amplitude. For modulation, the transducer amplitude $A \in [0, 1]$ was formulated as follows:

$$A = A^{max} A^{mod}, \quad (7)$$

where $A^{max} \in [0, 1]$ is the coefficient to manipulate final transducer amplitude. If $A^{max} = 0$, ultrasound is not outputted. If $A^{max} = 1$, the ultrasound is output with the maximum sound pressure. $A^{mod} \in [0, 1]$ is the coefficient to modulate the amplitude to present vibration sensations. A^{mod} is formulated as follows:

$$A^{mod} = A^{AM}(\lambda\Phi_1 + (1 - \lambda)\Phi_2) + 1 - A^{AM}, \quad (8)$$

$$\Phi_1 = \frac{1}{2}(\cos(2\pi f_1^{AM} t) + 1), \quad (9)$$

$$\Phi_2 = \frac{1}{2}(\cos(2\pi f_2^{AM} t) + 1), \quad (10)$$

where t is the elapsed time. $A^{AM} \in [0, 1]$ is the modulation amplitude. With $A^{AM} = 0$, only the LM stimulus with the constant amplitude was presented. $(f_1^{AM}, f_2^{AM}) = (30, 150)$ Hz is the modulation frequency. $\lambda \in [0, 1]$ is the allocation ratio of the modulation amplitude between the modulation frequencies. If $\lambda = 1$, the amplitude was modulated only at f_1^{AM} . If $\lambda = 0$, the amplitude was modulated only at f_2^{AM} . If $\lambda = 0.5$, the amplitude was modulated at both f_1^{AM} and f_2^{AM} with the same level. The simulation example of transducer amplitude A with eq. 8 is shown in Fig 4C. In the simulation, $(f_1^{AM}, f_2^{AM}) = (30, 150)$ Hz, $A^{AM} = 0.5, 1$, and $\lambda = 0, 0.5, 1$ were used.

We expected that the intensity of vibration sensation would increase with respect to the A^{AM} , and confirmed this expectation in Experiments 1 and 2.

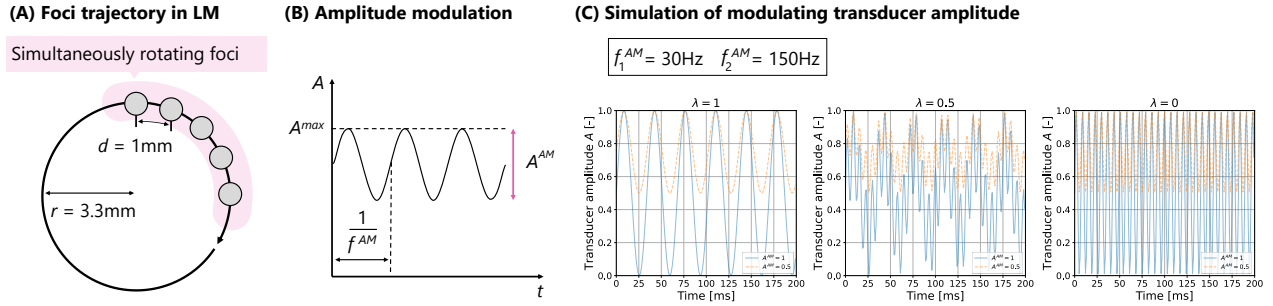


Fig. 4. Schematic illustration of ultrasound stimulation design. (A) LM in which 5 foci rotate at 5 Hz. (B) Variation of sound amplitude A with respect to modulation amplitude A^{AM} . (C) Simulated modulated transducer amplitude A . $f_1^{AM} = 30$ Hz and $f_2^{AM} = 150$ Hz were used for this simulation.

TABLE I
SUMMARY OF STIMULI USED IN THE EXPERIMENTS.

Stimulus	λ
S-30Hz	1
S-150Hz	0
S-Mix1	0.5
S-Mix2	0.7
S-LM	-

2) *Stimuli Used in Experiments*: We totally designed five stimuli by manipulating λ in eq. 8. The designed stimuli are summarized in Table I.

First, we designed an LM stimulus evoking pressure sensation only [27], [28]. The condition was $f^{LM} = 5$ Hz, $d = 1$ mm, and $r = 3.3$ mm. This LM stimulus without amplitude modulation was referred to as *S-LM*.

Second, for synthesizing vibration sensation, we designed four amplitude-modulated LM stimuli using eq. 8: *S-30Hz*, *S-150Hz*, *S-Mix1*, and *S-Mix2*. For all stimuli, the modulation frequency (f_1^{AM}, f_2^{AM}) = (30, 150) Hz was used. The $\lambda = 1$ and $\lambda = 0$ were used for *S-30Hz* and *S-150Hz*, respectively. The $\lambda = 0.5$ and $\lambda = 0.7$ were also used for *S-Mix1* and *S-Mix2*, respectively. The *S-Mix2*, in which the physical intensity of the 30 Hz vibration was higher than that of the 150 Hz vibration, was designed because the 30 Hz vibration was perceived as weaker than the 150 Hz vibration in our preliminary experiment. The modulation amplitude A^{AM} was varied from 1 to 0 in Experiment 1 and 2. In Experiment 3 and 4, different A^{AM} was used for each stimulus. The different A^{AM} design is described in Section VI-A.

We conducted sound pressure measurement and confirmed that desired stimulus was presented. The measurement setup and results were described in Supplemental file.

IV. EXP. 1: PERCEPTION THRESHOLD OF VIBRATION

This experiment evaluated the threshold of modulation amplitude A^{AM} for vibration perception to investigate whether the proposed method can synthesize vibration sensations to pressure sensations.

A. Setup and Stimulus

We used the tactile system introduced shown in Fig. 2. Participants operated this system while looking at the PC

display. The PC display presented both the virtual hand model of the participant's hand and a spherical VR object. A user interface (UI) for operating was also presented. Participants touched the VR object with the center of their right palm using a wrist and arm supporter as shown in Fig. 2B.

Four ultrasound tactile stimuli, *S-30Hz*, *S-150Hz*, *S-Mix1*, and *S-Mix2*, described in Section III-B2, were presented.

B. Procedure

14 males (12 in their 20s and 2 in their 30s) and 4 females (all in their 20s) participated in the experiment. All experiments conducted in this study were approved by the ethics committee at The University of Tokyo (Approval number: 24-626).

We used an interleaved staircase method to manipulate the modulation amplitude A^{AM} , and the A^{AM} varied from 0 to 1 by 0.02 according to the participant's response. Before the experiment, participants experienced the five stimuli: *S-LM*, *S-30Hz*, *S-150Hz*, *S-Mix1*, and *S-Mix2*. An ultrasound tactile stimulus was presented to the participant's palm for 1 s. After this stimulus, participants responded whether they perceived vibration with "yes" or "no". The stimulus presentation and the response were conducted by clicking buttons displayed on the PC display. In the ascending series, an initial A^{AM} was 0, corresponding to *S-LM* evoking pressure sensation only [27], [28]. If the response was "no" in this ascending series, the A^{AM} increased by 0.02 and the stimulus was presented again. This increase in the A^{AM} was repeated until the response reversed, i.e., until the participant perceived vibration. After the reversal, the A^{AM} started to decrease by 0.02. This decrease was repeated until the response reversed again. These experimental trials were repeated until the response reversed six times, and the A^{AM} at each reversal was recorded. In the descending series, an initial A^{AM} was the maximum value of 1, and the A^{AM} was decreased by 0.02 until the response reversed. After the reversal, A^{AM} started to increase until the response reversed again. The experimental trial was repeated until the response reversed six times, and A^{AM} at each reversal was recorded. The ascending and descending series were used in random order, and 12 A^{AM} at the response reversal was totally obtained. The average of the last three reversal A^{AM} values obtained in the ascending and descending series was calculated, and it was taken as the perceptual threshold. After

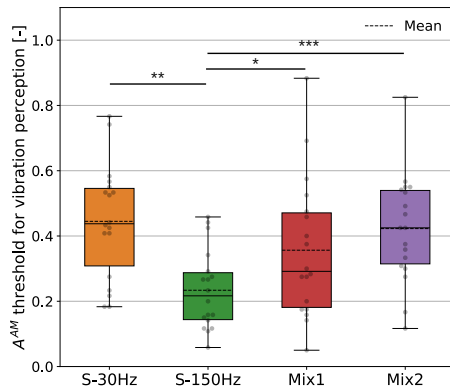


Fig. 5. Result of Experiment 1. Threshold modulation amplitude A^{AM} for vibration perception. These results indicate that participants were most sensitive to the vibration sensation in S-150Hz.

that, the stimulus condition was changed. The four stimulus conditions were used in random order.

C. Results and Analysis

Fig. 5 shows a boxplot of the thresholds of A^{AM} for vibration perception. The stimulus condition with the lowest perceptual threshold was S-150Hz, with an average of 0.23.

We conducted statistical analysis to evaluate the differences in the thresholds across the stimulus conditions. Since the results of the Shapiro-Wilk test indicated that all threshold data were normally distributed ($p > 0.05$), we used parametric analysis. The one-way repeated-measures ANOVA showed that the stimulus condition had a significant effect on perceptual threshold ($F(3, 51) = 8.82, p = 0.000083, \eta_p^2 = 0.34$). As a post-hoc test, we conducted a paired t-test with Holm correction. The results are shown in Fig. 5. The perceptual threshold of S-150Hz was significantly lower than that of all other stimulus conditions ($p < 0.05$). The p-value and Cohen's d was ($p = 0.0026, d = 1.43$), ($p = 0.00041, d = 1.33$), and ($p = 0.019, d = 0.72$) for [S-150Hz, S-30Hz], [S-150Hz, S-Mix2], and [S-150Hz, S-Mix1].

D. Discussion

These results indicated that vibration sensation was perceived by modulating the amplitude of ultrasound foci rotating.

The characteristic of the threshold was consistent with common vibration stimulus [41]. The threshold of S-150Hz was significantly lower than that of S-30Hz. A similar tendency has been observed in the common vibration generated using a vibrator.

The results of S-Mix1 and S-Mix2 indicated that adding a 30 Hz component increased the threshold of 150 Hz vibration. The perceptual threshold of S-Mix1 and S-Mix2 was significantly higher than that of S-150Hz.

V. EXP. 2: PERCEIVED INTENSITY

This experiment evaluated the perceived intensities of pressure and vibration sensations with respect to the variation of the modulation amplitude A^{AM} .

A. Setup and Stimulus

The setup for this experiment was the same as in Experiment 1. S-30Hz, S-150Hz, S-Mix1, and S-Mix2 described in Section III-B2, were presented. with the maximum A^{max} .

B. Procedure

14 males (12 in their 20s and 2 in their 30s) and 4 females (all in their 20s) participated in the experiment.

The ultrasound tactile stimuli with different A^{AM} were presented, and participants evaluated the vibration sensation intensity included in them. The evaluation was conducted with a 0–100 point visual analog scale (VAS). First, as a reference, a tactile stimulus with $A^{AM} = 1$ was presented to the palm for 1 s. Next, as a comparison stimulus, a tactile stimulus with a manipulated A^{AM} was presented for 1 s. The modulation type of the reference stimulus and the comparison stimulus was the same. To make participants focus only on the vibration sensation, the foci presented in the reference stimulus did not rotate. This A^{AM} was manipulated from 0 to 1 by 0.1 (in 11 steps) and used in random order. After experiencing these stimuli, participants evaluated the intensity of vibration sensation perceived in the comparison stimulus on a 0–100 point scale using a slider. A score of 100 corresponded to the vibration intensity of the reference stimulus, i.e., they reported 100 points if the perceived vibration intensity of the comparison stimulus was the same as that of the reference. If they perceived only pressure sensation without vibration, they reported 0 points. After using all steps of A^{AM} , the stimulus type was changed. The order of the stimulus type was random. Each participant reported the intensity of vibration sensation 44 times (4 stimulus types \times 11 steps of A^{AM} = 44 times).

After the vibration evaluation, participants evaluated the intensity of pressure sensation using a 0–100 point VAS. The S-LM was presented to the participant's palm for 1 s as a reference. The comparison stimuli were the same as those used for the evaluation of vibration sensation intensity. The A^{AM} was manipulated from 0 to 1 by 0.1 (in 11 steps). Participants reported the intensity of pressure sensation in the comparison stimulus on a 0–100 point scale using a slider. They were instructed to treat the pressure sensation intensity of the reference as 100. Each participant evaluated the intensity of pressure sensation 44 times (4 stimulus types \times 11 steps of A^{AM} = 44 times.)

C. Results and Analysis

Fig. 6A and B show the intensity variation of vibration and pressure sensation with respect to A^{AM} .

A Shapiro-Wilk test showed that the data at 43 out of 80 conditions did not normally distribute; thus, we applied the Friedman test to the data with the factor of A^{AM} . A^{AM} has a significant effect on the pressure and vibration intensity at all stimulus conditions. In vibration intensity, the p-values were $p = 2.2 \times 10^{-19}, 4.2 \times 10^{-27}, 7.6 \times 10^{-25}, 4.1 \times 10^{-23}$ for S-30Hz, S-150Hz, S-Mix1, and S-Mix2, respectively. In pressure intensity, the p-values were $p = 1.7 \times 10^{-12}, 2.9 \times 10^{-7}, 3.1 \times 10^{-9}, 5.2 \times 10^{-11}$ for S-30Hz, S-150Hz, S-Mix1, and S-Mix2, respectively.

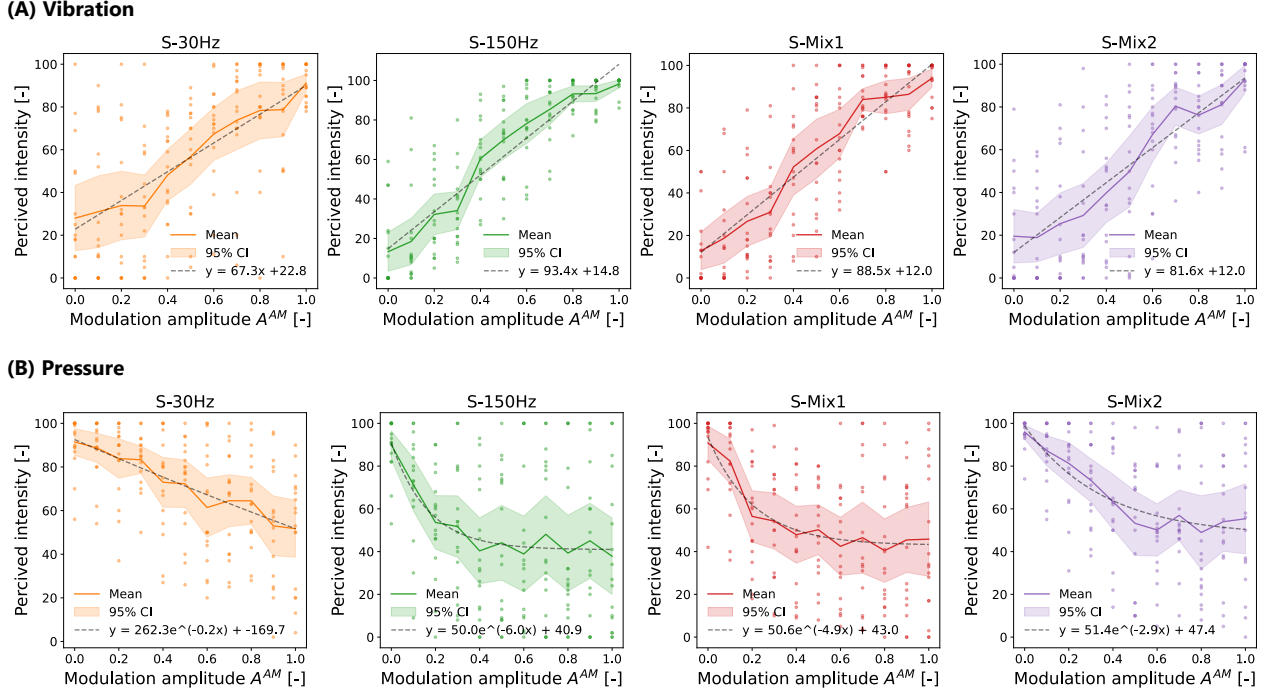


Fig. 6. Results of Experiment 2. (A) shows perceived intensity of vibration, and B) shows pressure sensations for modulation amplitude A^{AM} . These results indicate that the vibration sensation intensity of S-150Hz increased most rapidly, while its pressure sensation intensity decreased most rapidly.

These results indicated that as A^{AM} increased, vibration sensation intensity significantly increased while pressure sensation intensity significantly decreased.

We quantitatively evaluated the trends of vibration and pressure sensation intensities by fitting functions. First, a linear function was fitted to the vibration data. The fitted function is as follows:

$$I = aA^{AM} + b, \quad (11)$$

where I is the perceived intensity. Second, an exponential function was fitted to the pressure data since the averaged pressure sensation intensity decreased with the increase of A^{AM} , and the intensity stopped decreasing around 40 in S-150Hz, S-Mix1, and S-Mix2. The fitted function is as follows:

$$I = ce^{aA^{AM}} + b. \quad (12)$$

These fitted results are shown in Fig. 6. The a , coefficient of the A^{AM} . All R^2 values were higher than 0.9, indicating the functions were well fitted.

S-150Hz had the largest increase rate of the vibration sensation of $a = 93.4$, and S-30Hz had the lowest of $a = 67.3$. S-150Hz also had the largest decrease rate of the pressure sensation $a = -6$, and S-30Hz had the lowest $a = -0.17$.

D. Discussion

These results showed that the proposed method presents pressure and vibration sensations simultaneously, and that the intensity of vibration sensation can be controlled by A^{AM} .

The pressure sensation intensity decreased when the vibration sensation intensity increased, indicating a trade-off between the two sensations. This trade-off is attributed to the

acoustic power. When modulating sound pressure, the 5 Hz component of the acoustic power evoking pressure sensation was distributed to the 30 Hz and 150 Hz components, which may result in a decrease in pressure sensation intensity.

The slower decrease in pressure sensation intensity with S-30Hz may be due to the frequency characteristics of Merkel cells, the mechanoreceptors evoking pressure sensation. Since Merkel cells are more sensitive to 30 Hz than to 150 Hz [19], the increased 30 Hz power may have contributed to maintaining pressure sensation intensity.

Furthermore, these results are consistent with the perceptual threshold results obtained in Experiment 1 (shown in Fig. 5). Experiment 1 showed the perceptual threshold of A^{AM} in S-150Hz was the lowest, and Experiment 2 showed that the intensity of vibration sensation for S-150Hz most rapidly increased.

VI. EXP. 3: DISTINGUISHABLE STIMULUS

This experiment investigated how many types of distinguishable stimuli can be created by the proposed tactile synthesis method.

A. Setup and Stimulus

The setup for this experiment was the same as in Experiment 1 (shown in Fig. 2).

We designed six stimuli based on S-LM, S-30Hz, S-150Hz, and S-Mix2. To design stimuli with weak vibration sensation, we manipulated A^{AM} . As a strong vibration condition, $A^{AM} = 1$ was used for S-30Hz and S-150Hz. They were referred to as S-30Hz-s and S-150Hz-s (s: strong vibration).

TABLE II
SUMMARY OF STIMULI USED IN EXPERIMENT 3 AND 4.

Stimulus	A^{AM}
<i>S-LM</i>	0
<i>S-30Hz-w</i>	0.5
<i>S-30Hz-s</i>	1
<i>S-150Hz-w</i>	0.3
<i>S-150Hz-s</i>	1
<i>S-Mix2</i>	1

As a weak vibration condition, $A^{AM} = 0.5$ and $A^{AM} = 0.3$ were used for S-30Hz and S-150Hz. They were referred to as *S-30Hz-w* and *S-150Hz-w* (w: weak vibration). Because perceived vibration intensity at 150 Hz is higher than that at 30 Hz, as shown in Fig. 5 and 6, we used A^{AM} for S-30Hz that was larger than A^{AM} for S-150Hz. For S-Mix2, only $A^{AM} = 1$ was used. We only used S-Mix2, not S-Mix1, because we focused on stimuli with vastly different tactile sensations. In our preliminary study, the tactile sensation of S-Mix1 was similar to S-150Hz. We totally used six stimuli: S-LM, S-30Hz-w, S-30Hz-s, S-150Hz-w, S-150Hz-s, and S-Mix2, summarized in Table II.

B. Procedure

10 males (8 in their 20s and 2 in their 30s) and 2 females (all in their 20s) participated in the experiment.

Before the distinguish test, the maximum sound amplitude A^{max} was adjusted so that the perceived intensity was equal across stimuli for fair evaluation. In this adjustment phase, the reference stimulus was presented on the participant's palm, and then the comparison stimulus was presented. Participants adjusted the A^{max} of the comparison stimulus using a slider so that the perceived intensity of the comparison stimulus matched that of the reference. They can experience the standard and comparison stimuli as many times as they wanted. The reference was S-30Hz-s with $A^{max} = 0.9$. This condition was empirically employed because it was perceived as the weakest in our preliminary tests. The comparison stimuli were other five stimuli (S-LM, S-30Hz-w, S-150Hz-w, S-150Hz-s, and S-Mix2), and they were presented in random order. In the subsequent distinguish phase, this adjusted A^{max} was used for each condition. For S-30Hz-s, $A^{max} = 0.9$ was used.

In the distinguish phase, participants first clicked the "Reference Stimulus" button on the UI, and then they experienced the reference stimulus. As the reference, the six stimuli (described in Section VI-A) were presented randomly. Next, Participants clicked one of the buttons numbered 1–6 on the UI, and the participant experienced the comparison stimulus. The six stimuli were randomly assigned to the six buttons. After experiencing the stimuli, participants tried to find the stimulus identical to the reference among the six comparison stimuli. They can experience the reference and comparison stimuli as many times as they wanted. Each stimulus was presented for 0.5 s. The stimulus duration was set shorter than in Experiments 1 and 2 so that the participants can quickly switch stimuli many times. Each stimulus was presented twice in

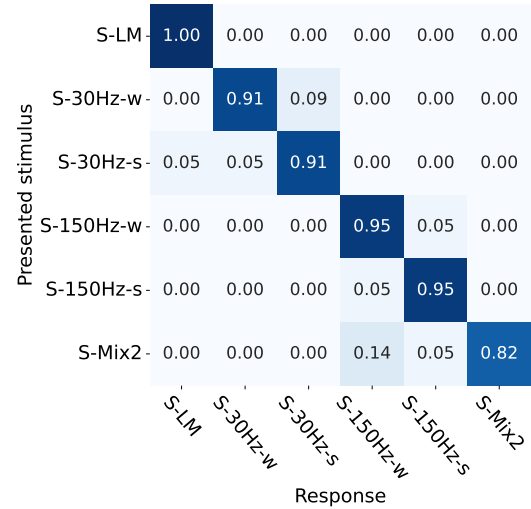


Fig. 7. Result of Experiment 3. Discrimination accuracy of the ultrasound stimulus.

random order as the reference. Thus, participants conducted 12 discrimination trials (6 stimuli \times 2 repetitions = 12).

C. Result

Fig. 7 shows the confusion matrix, showing the accuracy of the distinguished test. The accuracy of all stimulus conditions exceeded the chance level of 0.167. The highest distinguishing rate was 1.0, and the condition was S-LM. The lowest was 0.82, and the condition was S-Mix2.

D. Discussion

These results indicated that by synthesizing pressure and vibration sensations, at least six distinguishable stimuli can be created. Even when the synthesized vibration intensity was not maximum ($A^{AM} < 1$), the tactile sensation was still clearly distinguished. These findings indicated that the proposed method is effective in extending the displayable sensation in midair ultrasound haptics.

Furthermore, participants can distinguish S-Mix2 from other tactile stimuli, including single-frequency vibration sensations (i.e., S-30Hz and S-150Hz). This suggests that amplitude modulation with multiple frequencies can further extend the range of ultrasound tactile stimulus.

VII. EXP. 4: EVALUATING TEXTURE SENSATION

This experiment evaluates the sensation of roughness, stiffness, and friction sensations of the vibration-pressure-synthesized tactile stimuli by comparing them with real materials.

A. Setup and Stimulus

The setup for this experiment was the same as in Experiment 1 (Fig. 2).

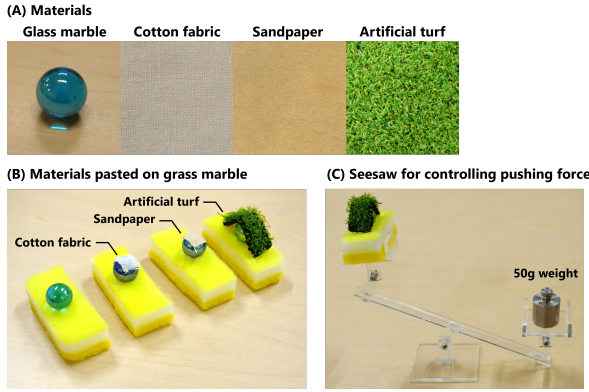


Fig. 8. Apparatus used in Experiment 4. (A) Four materials used. (B) Materials pasted on a glass marble. Participants stroked the pasted materials' surface with their palms. (C) An acrylic-made seesaw is used for controlling the pushing force of participants. A counterweight of 50 g was used.

The ultrasound stimuli for this experiment were the same as in Experiment 3. We used six stimuli: S-LM, S-30Hz-w, S-30Hz-s, S-150Hz-w, S-150Hz-s, S-Mix2, described in Section VI-A.

Four real materials shown in Fig. 8A were used for comparison with ultrasound stimuli: a glass marble, cotton fabric, sandpaper with a grit size of 100, and artificial turf. These materials were chosen so that each provides a different tactile sensation. For example, a glass marble was chosen to provide the smoothest sensation, while sandpaper was chosen to provide both a strong roughness and friction sensations.

The reason for choosing a glass marble was that its shape was close to the tactile shape of an ultrasound stimulus. Morisaki et al. showed that the perceived shape of S-LM is close to a sphere [28]. Other materials were pasted onto a glass marble so that their tactile shapes were close to that of this ultrasound tactile stimulus (shown in Fig. 8B).

B. Procedure

15 males (11 in their 20s and 4 in their 30s) and 4 females (all in their 20s) participated in the experiment.

Participants experienced the ultrasound tactile stimuli and real materials, and evaluated their sensation of roughness, stiffness, and friction sensations. The procedure was illustrated in Fig. 9. First, the participant stroked the real material with the left palm. Next, a spherical VR object moved 7 cm in the x-direction across the palm, and the corresponding stroking ultrasound stimulus was presented to the participant's right palm. The stroking speed of the ultrasound stimulus was 1.8 cm/s. This speed was selected based on preliminary experiments to ensure it felt like a natural stroke. Participants evaluated the roughness, stiffness, and friction sensations of the experienced ultrasound stimulus using a slider ranging from -100 to 100. A score of 0 corresponded to the same roughness, stiffness, and friction sensations as the real material. If participants judged that the ultrasound stimulus was rougher than the touched material, they rated the roughness of the stimulus between 1 and 100 points. Participants adjusted their stroking speed so that it matched the movement of the VR object. In the material

stroking, a contact force strength was controlled using a small seesaw shown in Fig. 8C. The real material was placed on this seesaw, and a 50 g weight was placed on the opposite side. Participants controlled their touch strength so that the seesaw did not move. The real materials were replaced manually by the experimenter. Participants can experience the real material and ultrasound stimuli up to three times.

As a control stimulus, a glass marble was used instead of an ultrasound stimulus. In this control condition, participants first stroked the real material as a standard stimulus, then stroked the glass marble as a comparison stimulus. Those strokes were performed with the left hand. After that, they evaluated the roughness, stiffness, and friction sensations of the glass marble on the -100 to 100 scale. In the case of comparison between glass marble, participants were instructed to respond with 0.

The real materials and ultrasound stimuli were presented in a random order. In total, participants experienced 28 times ((6 stimuli + 1 control) \times 4 materials = 28).

C. Results

Fig. 10 shows the evaluation results for roughness, stiffness, and friction sensations.

1) *Analysis of Roughness*: We analyzed the effect of the stimulus condition and the real material on the roughness data. Since a Shapiro-Wilk test showed the roughness data for comparison pairs of [S-LM, marble], [S-LM, sandpaper], and [marble, sandpaper] were not normally distributed ($p < 0.05$), after applying the aligned rank transformation (ART) to the data [42], a repeated two-way ANOVA was conducted. The results showed that the stimulus condition ($F(6, 108) = 48.7, p = 1.6 \times 10^{-28}, \eta_p^2 = 0.73$), the real material ($F(3, 54) = 74.1, p = 3.9 \times 10^{-19}, \eta_p^2 = 0.8$), and their interaction had significant effects ($F(18, 324) = 1.87, p = 0.017, \eta_p^2 = 0.094$). As the interaction effect was significant, we examined the simple main effects of stimulus condition and comparison material by applying a Friedman test with Holm correction to the data. The results showed that the stimulus condition had a significant effect on roughness at all real materials ($\chi^2(6), p < 0.0005$), and the real material had a significant effect on roughness at all stimulus conditions ($\chi^2(3), p < 0.0005$).

To examine differences in roughness between stimulus conditions, a Wilcoxon signed-rank test with Holm correction was applied to the roughness data for each material (shown in Fig. 10A). For all materials, the roughness of S-LM was significantly lower than that of all other stimuli except S-30Hz-w and the control. The roughness of S-150Hz-s was significantly higher than that of all other stimuli except S-150Hz-w and S-Mix2. These results are shown in Fig. 10A.

As additional analysis, the multiple comparisons were also conducted on the combined roughness data within materials and stimulus conditions shown in Fig. 10B. These results were also added to each corresponding graph.

These results indicated that the roughness sensation of the ultrasound stimulus was significantly increased by synthesizing vibration sensation.

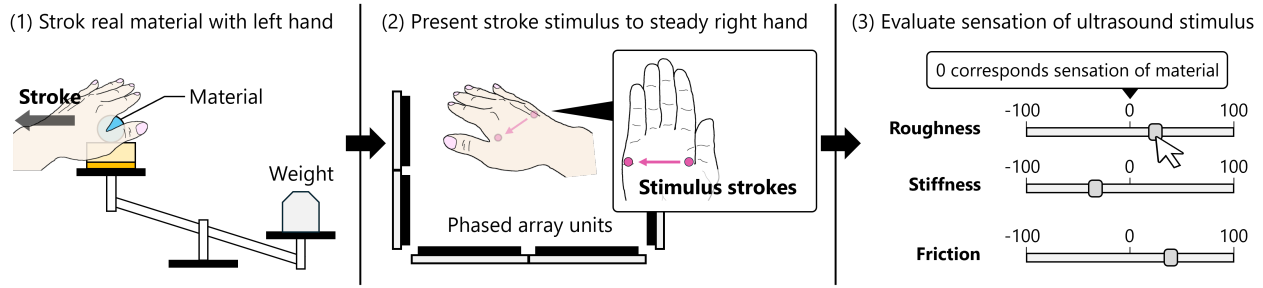


Fig. 9. Procedure of Experiment 4. (1) Participant stroked the real material with the left palm. (2) Next, a stroking ultrasound stimulus was presented to the participant's right palm. The stroking speed was 1.8 cm/s. (3) Participants evaluated the roughness, stiffness, and friction sensations of the experienced ultrasound stimulus using a slider ranging from -100 to 100. A score of 0 corresponded to the same roughness, stiffness, and friction sensations as the real material.

2) Analysis of Stiffness: We analyzed the stiffness data. Since a Shapiro-Wilk test showed the data for comparison pairs of [marble, artificial turf] was not normally distributed ($p < 0.05$), after applying ART to the data [42], a repeated two-way ANOVA was conducted. The results showed that the stimulus condition ($F(6, 108) = 13.5, p = 2.2 \times 10^{-11}, \eta_p^2 = 0.43$) and the real material ($F(3, 54) = 10.5, p = 1.6 \times 10^{-5}, \eta_p^2 = 0.37$) had significant effects. To examine the differences between stimulus conditions, a Wilcoxon signed-rank test with Holm correction was applied to the stiffness data for all materials shown in Fig. 10B. The stiffness of the glass marble (control stimulus) was significantly higher than that of all ultrasound stimuli ($p < 0.05$). The stiffness of S-150Hz-s was significantly higher than that of S-Mix2.

These results indicated that the stiffness of ultrasound stimuli was softer than that of a glass marble and that it did not vary significantly with respect to the synthesized vibration intensity.

3) Analysis of Friction: We analyzed the friction data. Since a Shapiro-Wilk test showed the data for comparison pairs of [S-Mix2, cotton], [S-LM, sandpaper] were not normally distributed ($p < 0.05$), after applying the ART to the data [42], a repeated two-way ANOVA was conducted. The results showed that the stimulus condition ($F(6, 108) = 8.3, p = 2.3 \times 10^{-7}, \eta_p^2 = 0.31$) and the real material ($F(3, 54) = 10.3, p = 1.8 \times 10^{-5}, \eta_p^2 = 0.36$) had significant effects. To examine the differences between stimulus conditions, a Wilcoxon signed-rank test with Holm correction was applied to the data. The friction sensation of S-150Hz-s was significantly higher than that of S-LM, S-30Hz-w, S-30Hz-s, and S-Mix2 ($p < 0.05$). The friction sensation of S-150Hz-w was also significantly higher than that of S-LM and S-30Hz-w.

These results indicated that synthesizing a 150 Hz vibration sensation significantly increased the friction sensation of ultrasound stimuli.

D. Discussion

These results demonstrated that pressure sensation evoked by ultrasound can create a smooth and slippery sensation, and its roughness and friction sensations were enhanced by synthesizing vibration sensations while maintaining its stiffness sensations. For enhancing roughness and sensation, 150 Hz vibration was more effective than 30 Hz vibration. Only

150 Hz vibration enhanced the friction sensation, while 30 Hz vibrations did not. The stiffness sensation was not varied among most stimulus conditions. To visualize the creatable sensation, the bubble chart of roughness and friction sensations is shown in Fig. 11. The medians were calculated from the data shown in Fig. 10B. The S-LM and glass marble were plotted in a separate area because their λ was undefined.

The following section discusses each sensation.

1) Roughness: By synthesizing vibrations, the roughness sensation was significantly enhanced as shown in Fig. 10A and B. This enhancement was consistent with the previous research [23], [24]. The previous studies showed that the roughness intensity increased as vibration intensity increased [24].

Considering the mechanism of roughness perception, the 30 Hz and 150 Hz vibration may create qualitatively different roughness sensations [20], [23]. When stroking a rough surface with different spatial frequencies, vibrations of different frequencies were caused on the fingertips. The frequency of the vibration increased as the surface spatial frequency increased. Therefore, S-30Hz and S-150Hz likely conveyed textures of lower spatial and higher spatial frequency, respectively.

To examine real materials corresponding to the produced roughness sensations, we applied one-sample Wilcoxon signed-rank tests with Holm correction to the roughness data (shown in Fig. 10A). We confirmed whether the roughness scores were significantly different from zero. There was no significant difference between S-LM and a glass marble, nor between S-150Hz-s and sandpaper ($p > 0.05$).

2) Stiffness: The stiffness sensation of ultrasound stimuli was softer than that of a glass marble, and it was not significantly varied among all stimulus conditions except for [S-150H, Mix2]. The lack of variation in the stiffness sensation may be due to the fact that the maximum sound amplitude A_{max} was always constant between the stimulus conditions.

Although the stiffness of the ultrasound stimulus was softer than that of a glass marble, the difference was lower than 30 in the median and not huge. Considering that the participants were allowed to apply up to 50 gf of force when stroking, the ultrasound stimulus may not be extremely soft, and it may feel like contact with a physical object.

The stiffness of the ultrasound stimulus was judged entirely through a passive situation, which may have influenced the results. Ultrasound stimuli were presented to a stationary palm

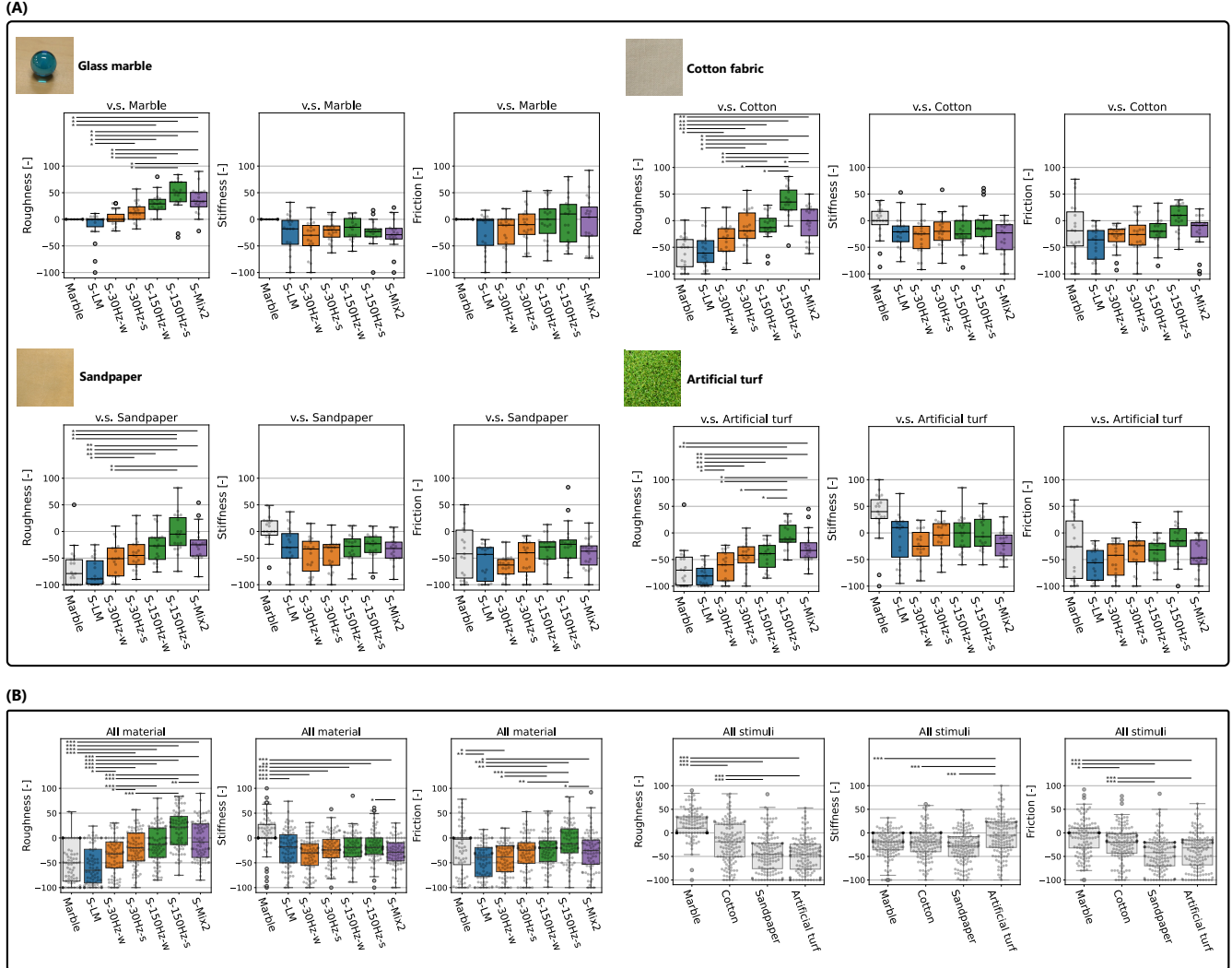


Fig. 10. Result of Experiment 4. Comparison result of roughness, stiffness, and friction sensation. (A) Evaluation results for each real material. The results of the pairwise comparison are also shown. This comparison was conducted only on roughness data. *, **, and *** indicates $p < 0.05$, $p < 0.005$, $p < 0.0005$, respectively. (B) The left graph shows the combined data for all materials. The right graph shows the combined data for the stimulus condition. The results of the pairwise comparison are also shown.

with the same stimulus size (focus size). In contrast, when evaluating the stiffness of real materials, participants actively touched the object and could use changes in contact area between the hand and the materials as a stiffness cue.

We confirmed whether the stiffness scores differed from zero using a Wilcoxon signed-rank test with Holm correction. There was no significant difference in the stiffness between all stimuli except for S-Mix2 and the artificial turf ($p > 0.05$).

3) *Friction*: The friction sensation of the ultrasound stimulus was significantly enhanced by synthesizing a 150 Hz vibration. This friction enhancement was consistent with the perceptual mechanism of friction through vibration. When stroking the surface of an object, depending on its coefficient of friction, the fingertip alternately slips and sticks at several hundred Hz. The frictional vibration at several hundred Hz contributes to the friction sensation [25], [26]. The synthesized 150 Hz vibration in the ultrasound stimulus may play the role of such frictional vibrations, thereby enhancing the friction sensation. The 30 Hz vibration did not significantly enhance

friction sensation, likely because its frequency order of 30 Hz differed from that of typical frictional vibration.

Finally, we confirmed whether the friction scores differed from zero using a Wilcoxon signed-rank test with Holm correction. There was no significant difference in the stiffness between S-150Hz-s and [the glass marbles, cotton fabric, and artificial turf] ($p > 0.05$).

VIII. LIMITATION AND FUTURE WORK

A. Displayable Sensation with Proposed Method

With the proposed rendering method, reproducing the tactile sensation of objects with high friction and low roughness is difficult. Synthesizing a 150 Hz vibration was necessary to enhance friction sensation, but in this case, roughness sensation was also significantly enhanced. We will explore a method to selectively enhance the sensation of friction.

The perception of stiffness was limited to the level of artificial turf with the proposed method. As a possible solution

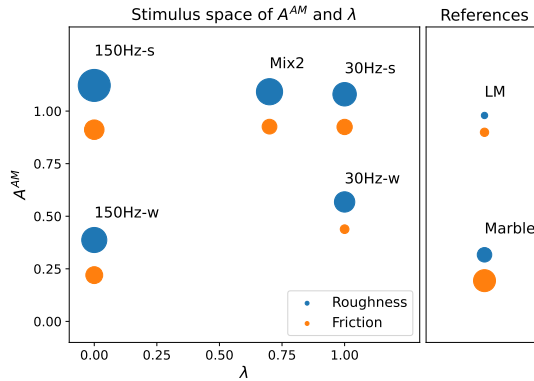


Fig. 11. Renderable tactile sensation of the proposed method visualized with A^AM and λ . The circle size indicates the median value of roughness and friction data shown in Fig. 10B. S-LM and glass marble were plotted in a separate area because their λ was undefined.

for this, previous studies have proposed enhancing the stiffness sensation in ultrasound tactile stimulus by dynamically varying the stimulus presentation area according to finger movement [43]. We will combine this stimulus area variation method with the proposed method to expand the range of displayable stiffness sensations.

Our approach excluded SA-II (slowly adaptive type II) components. Although SA-II receptor primarily react shear force stimulus, current ultrasound midair haptics cannot cover such stimulus [44].

B. Experimental Design

In Experiment 4, participants actively stroked real materials, but an ultrasound stimulus was presented to steady participants' hands, corresponding to a passive touch situation. This difference in the touch situation may have influenced the evaluation results. We will evaluate this effect.

In Experiment 4, the frequency of the vibration stimulus and the stimulus movement speed were constant. Since roughness perception relies on the vibration frequency perceived when stroking an object surface, changing this frequency and the movement speed may alter the roughness sensation [20], [23]. We will evaluate these effects in the future.

IX. CONCLUSION

This study proposes a midair tactile rendering method synthesizing three basic ultrasound stimulus: static pressure, 30 Hz vibration, and 200 Hz vibration, primarily stimulating SA-I, FA-I, and FA-II receptors, respectively. The pressure stimulus was presented with a 5 Hz ultrasound foci rotation, while vibration stimuli were synthesized by modulating the sound amplitude of the foci.

The proposed method can render at least six distinguishable tactile texture with different roughness and friction sensations. The pressure-only stimulus felt smooth and slippery, and its smoothness was close that of glass marble. The synthesized vibration enhanced its roughness and friction sensations, and its roughness reached that of a 100 grid sandpaper.

REFERENCES

- [1] T. Iwamoto, M. Tatezono, and H. Shinoda, "Non-contact method for producing tactile sensation using airborne ultrasound," in *Proceedings of International Conference on Human Haptic Sensing and Touch Enabled Computer Applications*. Springer, 2008, pp. 504–513.
- [2] T. Hoshi, M. Takahashi, T. Iwamoto, and H. Shinoda, "Noncontact tactile display based on radiation pressure of airborne ultrasound," *IEEE Transactions on Haptics*, vol. 3, no. 3, pp. 155–165, 2010.
- [3] T. Carter, S. A. Seah, B. Long, B. Drinkwater, and S. Subramanian, "Ultrahaptics: multi-point mid-air haptic feedback for touch surfaces," in *Proceedings of the 26th annual ACM symposium on User interface software and technology*. ACM, 2013, pp. 505–514.
- [4] K. Yosioka and Y. Kawasima, "Acoustic radiation pressure on a compressible sphere," *Acta Acustica united with Acustica*, vol. 5, no. 3, pp. 167–173, 1955.
- [5] I. Rakkolainen, E. Freeman, A. Sand, R. Raisamo, and S. Brewster, "A survey of mid-air ultrasound haptics and its applications," *IEEE Transactions on Haptics*, vol. 14, no. 1, pp. 2–19, 2020.
- [6] Y. Monnai, K. Hasegawa, M. Fujiwara, K. Yoshino, S. Inoue, and H. Shinoda, "Haptomime: mid-air haptic interaction with a floating virtual screen," in *Proceedings of the 27th annual ACM symposium on User interface software and technology*, 2014, pp. 663–667.
- [7] P. I. Cornelio Martinez, S. De Pirro, C. T. Vi, and S. Subramanian, "Agency in mid-air interfaces," in *Proceedings of the 2017 CHI Conference on Human Factors in Computing Systems*, 2017, pp. 2426–2439.
- [8] G. Young, H. Milne, D. Griffiths, E. Padfield, R. Blenkinsopp, and O. Georgiou, "Designing mid-air haptic gesture controlled user interfaces for cars," *Proceedings of the ACM on human-computer interaction*, vol. 4, no. EICS, pp. 1–23, 2020.
- [9] G. Korres, S. Chehabeddine, and M. Eid, "Mid-air tactile feedback co-located with virtual touchscreen improves dual-task performance," *IEEE Transactions on Haptics*, vol. 13, no. 4, pp. 825–830, 2020.
- [10] S. Suzuki, M. Fujiwara, Y. Makino, and H. Shinoda, "Midair hand guidance by an ultrasound virtual handrail," in *Proceedings of 2019 IEEE World Haptics Conference (WHC)*, IEEE. IEEE, 2019, pp. 271–276.
- [11] A. Yoshimoto, K. Hasegawa, Y. Makino, and H. Shinoda, "Midair haptic pursuit," *IEEE Transactions on Haptics*, vol. 12, no. 4, pp. 652–657, 2019.
- [12] E. Freeman, D.-B. Vo, and S. Brewster, "Haptiglow: Helping users position their hands for better mid-air gestures and ultrasound haptic feedback," in *Proceedings of 2019 IEEE World Haptics Conference (WHC)*. IEEE, 2019, pp. 289–294.
- [13] K. Tsumoto, T. Morisaki, M. Fujiwara, Y. Makino, and H. Shinoda, "Presentation of tactile pleasantness using airborne ultrasound," in *Proceedings of 2021 IEEE World Haptics Conference (WHC)*, IEEE. IEEE, 2021, pp. 602–606.
- [14] E. Freeman, R. Anderson, J. Williamson, G. Wilson, and S. A. Brewster, "Textured surfaces for ultrasound haptic displays," in *Proceedings of the 19th ACM international conference on multimodal interaction*, 2017, pp. 491–492.
- [15] D. Ablart, W. Frier, H. Limerick, O. Georgiou, and M. Obrist, "Using ultrasonic mid-air haptic patterns in multi-modal user experiences," in *2019 IEEE International Symposium on Haptic, Audio and visual Environments and games (HAVE)*. IEEE, 2019, pp. 1–6.
- [16] E. Sakiyama, A. Matsubayashi, D. Matsumoto, M. Fujiwara, Y. Makino, and H. Shinoda, "Midair tactile reproduction of real objects," in *Proceedings of International Conference on Human Haptic Sensing and Touch Enabled Computer Applications*. Springer, 2020, pp. 425–433.
- [17] E. Freeman, "Enhancing ultrasound haptics with parametric audio effects," in *Proceedings of the 2021 International Conference on Multimodal Interaction*, 2021, pp. 692–696.
- [18] J. Hosoi, D. Jin, Y. Ban, and S. Warisawa, "Voluminous fur stroking experience through interactive visuo-haptic model in virtual reality," *IEEE Transactions on Haptics*, 2024.
- [19] S. J. Bolanowski Jr, G. A. Gescheider, R. T. Verrillo, and C. M. Checkosky, "Four channels mediate the mechanical aspects of touch," *The Journal of the Acoustical society of America*, vol. 84, no. 5, pp. 1680–1694, 1988.
- [20] M. Konyo, S. Tadokoro, A. Yoshida, and N. Saiwaki, "A tactile synthesis method using multiple frequency vibrations for representing virtual touch," in *Proceedings of 2005 IEEE/RSJ International Conference on Intelligent Robots and Systems*. IEEE, 2005, pp. 3965–3971.
- [21] V. Yem and H. Kajimoto, "Wearable tactile device using mechanical and electrical stimulation for fingertip interaction with virtual world,"

in *Proceedings of 2017 IEEE Virtual Reality (VR)*. IEEE, 2017, pp. 99–104.

[22] Y. Huang, J. Zhou, P. Ke, X. Guo, C. K. Yiu, K. Yao, S. Cai, D. Li, Y. Zhou, J. Li *et al.*, “A skin-integrated multimodal haptic interface for immersive tactile feedback,” *Nature Electronics*, vol. 6, no. 12, pp. 1020–1031, 2023.

[23] S. J. Bensmaia and M. Hollins, “The vibrations of texture,” *Somatosensory & motor research*, vol. 20, no. 1, pp. 33–43, 2003.

[24] M. Natsume, Y. Tanaka, W. M. B. Tiest, and A. M. Kappers, “Skin vibration and contact force in active perception for roughness ratings,” in *2017 26th IEEE International Symposium on Robot and Human Interactive Communication (RO-MAN)*. IEEE, 2017, pp. 1479–1484.

[25] S. Guest, A. Mehrabyan, G. Essick, N. Phillips, A. Hopkinson, and F. McGlone, “Physics and tactile perception of fluid-covered surfaces,” *Journal of texture studies*, vol. 43, no. 1, pp. 77–93, 2012.

[26] Y. Nonomura, T. Fujii, Y. Arashi, T. Miura, T. Maeno, K. Tashiro, Y. Kamikawa, and R. Monchi, “Tactile impression and friction of water on human skin,” *Colloids and Surfaces B: Biointerfaces*, vol. 69, no. 2, pp. 264–267, 2009.

[27] T. Morisaki, M. Fujiwara, Y. Makino, and H. Shinoda, “Non-vibratory pressure sensation produced by ultrasound focus moving laterally and repetitively with fine spatial step width,” *IEEE Transactions on Haptics*, vol. 15, no. 2, pp. 441–450, 2021.

[28] —, “Noncontact haptic rendering of static contact with convex surface using circular movement of ultrasound focus on a finger pad,” *IEEE Transactions on Haptics*, vol. Early Access, 2023.

[29] T. Morisaki and Y. Ujitoko, “Towards intensifying perceived pressure in midair haptics: Comparing perceived pressure intensity and skin displacement between $1m$ and am stimuli,” *Eurohaptics 2024*, vol. In Press, 2024.

[30] D. Beattie, W. Frier, O. Georgiou, B. Long, and D. Ablart, “Incorporating the perception of visual roughness into the design of mid-air haptic textures,” in *Proceedings of ACM Symposium on Applied Perception 2020*, 2020, pp. 1–10.

[31] R. Montano-Murillo, D. Pittéra, W. Frier, O. Georgiou, M. Obrist, and P. Cornelio, “It sounds cool: Exploring sonification of mid-air haptic textures exploration on texture judgments, body perception, and motor behaviour,” *IEEE Transactions on Haptics*, vol. 17, no. 2, pp. 237–248, 2023.

[32] J. Xue, R. Montano Murillo, C. Dawes, W. Frier, P. Cornelio, and M. Obrist, “Fabsound: audio-tactile and affective fabric experiences through mid-air haptics,” in *Proceedings of the 2024 CHI Conference on Human Factors in Computing Systems*, 2024, pp. 1–17.

[33] L. Mulot, G. Gicquel, Q. Zanini, W. Frier, M. Marchal, C. Pacchierotti, and T. Howard, “Dolphin: A framework for the design and perceptual evaluation of ultrasound mid-air haptic stimuli,” in *Proceedings of ACM Symposium on Applied Perception 2021*, 2021, pp. 1–10.

[34] H. Seifi, S. Chew, A. J. Nascè, W. E. Lowther, W. Frier, and K. Hornbæk, “Feelillustrator: A design tool for ultrasound mid-air haptics,” in *Proceedings of the 2023 CHI Conference on Human Factors in Computing Systems*, 2023, pp. 1–16.

[35] C. Lim, G. Park, and H. Seifi, “Designing distinguishable mid-air ultrasound tactons with temporal parameters,” in *Proceedings of the 2024 CHI Conference on Human Factors in Computing Systems*, 2024, pp. 1–18.

[36] T. Morisaki, M. Fujiwara, Y. Makino, and H. Shinoda, “Midair haptic-optic display with multi-tactile texture based on presenting vibration and pressure sensation by ultrasound,” in *Proceedings of SIGGRAPH Asia 2021 Emerging Technologies*, 2021, pp. 1–2.

[37] S. Suzuki, S. Inoue, M. Fujiwara, Y. Makino, and H. Shinoda, “Autd3: Scalable airborne ultrasound tactile display,” *IEEE Transactions on Haptics*, vol. 14, no. 4, pp. 740–749, 2021.

[38] Z. Shen, M. K. Vasudevan, J. Kućera, M. Obrist, and D. Martinez Plasencia, “Multi-point stm: Effects of drawing speed and number of focal points on users’ responses using ultrasonic mid-air haptics,” in *Proceedings of the 2023 CHI Conference on Human Factors in Computing Systems*, 2023, pp. 1–11.

[39] Z. Shen, Z. Morgan, M. K. Vasudevan, M. Obrist, and D. Martinez Plasencia, “Controlled-stm: a two-stage model to predict user’s perceived intensity for multi-point spatiotemporal modulation in ultrasonic mid-air haptics,” in *Proceedings of the 2024 CHI conference on human factors in computing systems*, 2024, pp. 1–12.

[40] D. Hajas, D. Pittéra, A. Nasce, O. Georgiou, and M. Obrist, “Mid-air haptic rendering of 2d geometric shapes with a dynamic tactile pointer,” *IEEE Transactions on Haptics*, vol. 13, no. 4, pp. 806–817, 2020.

[41] A. B. Vallbo, R. S. Johansson *et al.*, “Properties of cutaneous mechanoreceptors in the human hand related to touch sensation,” *Hum neurobiol*, vol. 3, no. 1, pp. 3–14, 1984.

[42] J. O. Wobbrock, L. Findlater, D. Gergle, and J. J. Higgins, “The aligned rank transform for nonparametric factorial analyses using only anova procedures,” in *Proceedings of the SIGCHI conference on human factors in computing systems*, 2011, pp. 143–146.

[43] Q. Sun, M. Zhang, Y. Makino, and H. Shinoda, “Expanding softness and hardness sensations in mid-air ultrasonic haptic interfaces combining amplitude and spatiotemporal modulation,” *IEEE Access*, vol. 12, pp. 154 743–154 750, 2024.

[44] R. S. Johansson and Å. B. Vallbo, “Tactile sensory coding in the glabrous skin of the human hand,” *Trends in neurosciences*, vol. 6, pp. 27–32, 1983.